Unfolding pathway and its identifiability in heterogeneous chains of bistable units

Manon Benedito, Stefano Giordano

Unfolding pathway and its identifiability in heterogeneous chains of bistable units

Manon Benedito, Stefano Giordano*

Univ. Lille, CNRS, Centrale Lille, ISEN, Univ. Valenciennes, LIA LICS/LEMAC, UMR 8520 - IEMN - Institute of Electronics, Microelectronics and Nanotechnology, F-59000 Lille, France

Abstract

We investigate the behavior of a chain of bistable units with an heterogeneous distribution of energy jumps between the folded and unfolded states. For homogeneous chains, loaded by soft or hard devices, all units at each switching occurrence have the same probability to unfold and it is therefore impossible to identify an unfolding pathway. Conversely, the heterogeneity represents a quenched disorder from the statistical mechanics point of view, and is able to break the symmetry eventually generating an unfolding pathway. We prove that the most probable pathway is realized by arranging the energy jumps in ascending order. Hence, the mechanics of this system is able to implement a statistical sorting procedure. We quantitatively evaluate the identifiability of the obtained unfolding pathway in terms of the variance of the heterogeneous energy jumps and the temperature. This concept is applied to both deterministic and random distributions of energy jumps within the chain.

Keywords: bistable chains, unfolding pathway, heterogeneity, statistical ensembles

1. Introduction

Chains of bistable or multistable units – with coexisting potential energy minima - have recently garnered a wide interest because of their capability to represent the behavior of several macromolecules of biological origin and of materials or structures with internal transitions, typically generated by micro instabilities.

Concerning the biological macromolecules, the bistability has been observed by force-spectroscopy experiments [1–5], typically performed on polypeptides [6–8], RNA [9, 10], and DNA [11–14]. The observation of these complex behaviors is very important to validate the statistical mechanical theories describing the thermo-mechanics of polymer chains [15–19]. The modeling of bistable systems is also relevant for the understanding of the muscles operating principle [20, 21]. In this case, bistable mechanical models are able to describe the physical mechanisms of the two passive and active muscle regimes. In several artificial systems, the bistability has been exploited to obtain particular performances. We can cite bistable mechanical metamaterials with a negative Poisson ratio (auxetic media) [22] or systems for controlling the waves propagation [23]. Moreover, asymmetric energy barriers (representing a mechanical diode effect) can be realized through origami structures, which may be used as building blocks for solids with unique functionalities [24]. Similarly, architected materials (with internal instabilities) have been proposed to improve the energy dissipation, which is crucial for having a good damage tolerance [25]. Models based on chains of bistable units with transitions between two states have been also adopted to model plasticity, hysteretic behaviors and martensitic transformations in continuum mechanics [26–32].

The paradigmatic minimal model for describing all these physical situations is constituted of a chain of bistable units that may assume two states, classically named folded and unfolded configurations. The bimodal energy potential of each unit is therefore composed of two energy wells with different basal energies, separated by a given energy barrier. This chain is typically considered at a given temperature T in order to study the effect of the thermal fluctuations on the transitions statistics between the states. When the chain is homogeneous (all units have the same properties), the system behavior has been studied in detail. Indeed, it is well known that the thermo-mechanical response of this chain is strongly dependent on the applied boundary conditions (see Fig.1a for details). When we apply a given force (isotensional condition imposed by soft devices), the system is in the Gibbs ensemble of the statistical mechanics and the force-extension response is characterized by a plateau describing the simultaneous transitions of all the units. On the other hand, when we prescribe the extension of the chain (isometric condition imposed by hard devices), the system is in the Helmholtz ensemble of the statistical mechanics and the force-extension response is characterized by a series of peaks representing the sequential unfolding of the units. Moreover, the intermediate cases, in-between the Gibbs and the Helmholtz ensembles, have been recently studied by introducing the real stiffness of the adopted devices [8]. These results can be obtained with the method of the spin variables, which introduces a discrete variable (spin-like) for each unit, able to define the potential well explored by the unit itself (folded or unfolded state) [33–36]. This approach, originally introduced to develop a chemo-mechanical model of the muscle behavior [37, 38], has

*Corresponding author

Email address: stefano.giordano@univ-lille.fr (Stefano Giordano)

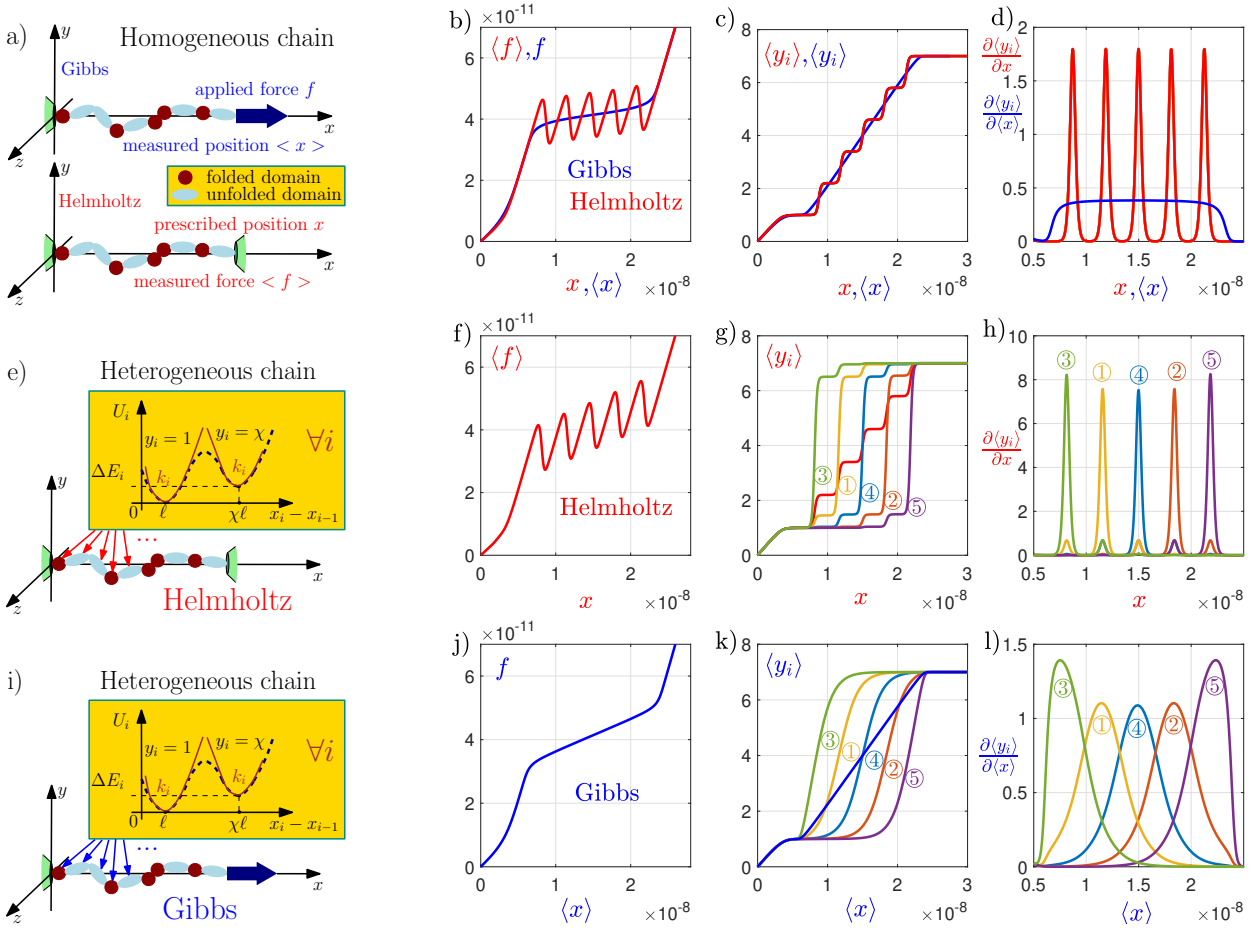

Figure 1: Folding and unfolding processes in homogeneous and heterogeneous chains. Panel a): Gibbs (isotensional) and Helmholtz (isometric) conditions applied to homogeneous chains. Panel b): Force-extension response (homogeneous chain) for isotensional condition (with a force plateau, blue) and isometric condition (sawtooth like, red). Panel c): average spin variables showing a synchronous unfolding in the Gibbs ensemble and a sequential unfolding in the Helmholtz one (homogeneous chain). All spins have the same behavior, and therefore all units have the same probability to unfold at each switching occurrence (no unfolding pathway can be identified). Panel d): plot of the quantities $\partial\langle y_i \rangle/\partial x$ (or $\partial\langle y_i \rangle/\partial\langle x\rangle$) versus x (or $\langle x\rangle$) for homogeneous chains. These functions are proportional to the probability density of the position at which we can observe the unfolding transition of the i-th unit. Panel e): Scheme of an heterogeneous chain under isometric condition where the units have different ΔE_i (energy jumps) and k_i (elastic constants). Panel f): Helmholtz force-extension response, slightly modified by the introduction of the heterogeneity. Panel g): the average spin variables under isometric condition show the unfolding pathway of the process corresponding to the ascending order of the values ΔE_i: ③,①,④,②,⑤ (in this example $\Delta E_3 < \Delta E_1 < \Delta E_4 < \Delta E_2 < \Delta E_5$). Red curve: mean value $\frac{1}{N}\sum\langle y_i \rangle$ of the averaged spins. Panel h): plot of the quantities $\partial\langle y_i \rangle/\partial x$, confirming the symmetry breaking induced by the heterogeneity. Panel i): scheme of an heterogeneous chain under isotensional condition where the units have different ΔE_i (energy jumps) and k_i (elastic constants). Panel j): Gibbs force-extension response, slightly modified by the introduction of the heterogeneity. Panel k): the average spin variables under isotensional condition show the unfolding pathway of the process corresponding to the ascending order of the values ΔE_i: ③,①,④,②,⑤ (in this example $\Delta E_3 < \Delta E_1 < \Delta E_4 < \Delta E_2 < \Delta E_5$, as before). Blue curve: mean value $\frac{1}{N}\sum\langle y_i \rangle$ of the averaged spins. Panel l): plot of the quantities $\partial\langle y_i \rangle/\partial\langle x\rangle$, confirming the symmetry breaking induced by the heterogeneity. We adopted the following parameters: $N = 5$, $\ell = 0.5$nm, $T = 300$K, $\chi = 7$, $k_i = 0.04$N/m $\forall i$, $\Delta E_i = 30 K_B T$ $\forall i$ in the homogeneous chain and $\Delta E_1 = 27.5 K_B T$, $\Delta E_2 = 32.5 K_B T$, $\Delta E_3 = 25 K_B T$, $\Delta E_4 = 30 K_B T$, $\Delta E_5 = 35 K_B T$ in the heterogeneous case.

been exploited only for homogeneous chains. Therefore, the main aim of the present investigation is to extend these methods to the case of heterogeneous units, namely with heterogeneous energy jumps between the states and heterogeneous elastic stiffness of the units. The most important difference between the homogeneous and the heterogeneous cases can be discussed by observing the behavior of the system within both the Gibbs and the Helmholtz ensembles. We suppose to increase gradually the force applied or the extension prescribed to a homogeneous chain. We observe a progressive unfolding of the units. However, because of the homogeneity of the chain, we can not say what unit unfolds at each transition occurrence. Indeed, all units have the same probability to unfold at each transition. Conversely, if the chain is heterogeneous with respect to the energy difference between folded and unfolded states of the units, we are able to identify an unfolding pathway, which is the sequence of the unfolding processes. The heterogeneity, representing a quenched disorder within the system, is able to break the symmetry among the units and to generate different unfolding probabilities at each transition, eventually producing an unfolding pathway. We remark that the process corresponding to the complete unfolding of a chain is a probabilistic event and therefore the observed pathway assumes a statistical character. It means that if we repeat the experiment many times, we can observe, as a result, different unfolding pathways. However, the heterogeneity defines different probabilities for each pathway and therefore is able to identify the most probable unfolding pathway for a given chain. It is worth noticing that the symmetry breaking can be also obtained with non-local interactions between the units of the chain [39, 40]. In this Letter, we propose a mathematical model explaining the origin of the symmetry breaking in heterogeneous chains and we prove that the unfolding pathway is described by the ascending order of the energy jumps between folded and unfolded states. It means that the system implements a statistical sorting procedure. To give a complete picture of this process, we also define and apply the concept of identifiability of the unfolding pathway. This concept is based on the statistical character of the (in general nonunique) unfolding pathway and quantifies to what extend it is possible to determine the most probable pathway, i.e. the most likely observed sequence of unfolding processes in a given experiment. We discuss some examples based on deterministic and random sequences of heterogeneous energy jumps, to show the generation of an unfolding pathway and the meaning of its identifiability.

2. The Gibbs ensemble

We consider a one-dimensional chain aligned with the x-axis of a reference frame and made of N units, which are bistable (in each direction, $x > 0$ and $x < 0$) and therefore can be either folded or unfolded (in each direction). We consider a unit length ℓ in the folded state and a length $\chi\ell$ in the unfolded one ($\chi > 1$). The potential energy of the units is described by

$$U_i(x, y_i) = v_i(y_i) + \frac{1}{2}k_i\,(x - y_i\ell)^2\,, \tag{1}$$

where $v_i(\pm 1) = 0$ and $v_i(\pm\chi) = \Delta E_i$ are the energy jumps between folded and unfolded states (arbitrarily varying with i). The parameters k_i represent the elastic constants of the units, which are independent of the folded or unfolded state but possibly heterogeneous along the chain. Moreover, y_i is the spin variable and assumes the values in $\mathcal{S} = \{\pm 1, \pm\chi\}$. The value of $y_i \in \mathcal{S}$ allows the identification of the energy well (quadratic potential) explored by the i-th unit (see Fig.3 in Ref.[33]). We remark that the potential energy in Eq.(1) is symmetric with respect to the coordinate x, thus describing the folding-unfolding process in both direction of $x > 0$ and $x < 0$ [33].

While the model should be three-dimensional to exactly represent, e.g., the behavior of real macromolecules, we adopt a one-dimensional scheme for the sake of simplicity. In this regard, the passage at $x = 0$ is somewhat unphysical, but we will study extensions and forces only in the positive direction. Since we consider a one-dimensional system, we introduced four potential wells (two folded and two unfolded). Indeed, the consideration of positive and negative orientations of the elements allows modeling entropic, enthalpic, unfolding and overstretching regimes, as discussed in Ref.[33]. It is also important to underline that the approximation introduced by the spin variables allows us to perform an analytic study of the system under the hypothesis of thermodynamic equilibrium [33–35, 37, 38]. However, if we consider the out-of-equilibrium regime, the dynamics of the folding-unfolding process is also influenced by the energy barrier between the states, as classically described by the reaction-rate Kramers theory [41]. Concerning the Gibbs ensemble (isotensional condition imposed by soft devices), the total potential energy of the one-dimensional system is given by

$$U_G\,(\vec{x}, \vec{y}, f) = \sum_{i=1}^{N} U_i\,(x_i - x_{i-1}, y_i) - f x_N - \sum_{i=1}^{N} g_i y_i, \tag{2}$$

where $x_0 = 0$ and f is the force applied to the last element of the chain. Here, we defined $\vec{x} = (x_1, ..., x_N) \in \mathbb{R}^N$ and $\vec{y} = (y_1, ..., y_N) \in \mathcal{S}^N$. Moreover, the quantities g_i represent an external field $\vec{g}$ directly acting on the configurational state of the elements (it acts as a chemical potential) [34]. While we will consider $\vec{g} = 0$ in the applications described in this Letter, the vector $\vec{g}$ is very important from the mathematical point of view, to easily calculate the heterogeneous average values of the spin variables (see Eqs.(7) and (11) below). Therefore, we can write the partition function in the Gibbs ensemble by summing the discrete spins and integrating the continuous coordinates

$$Z_G(f) = \sum_{y_1 \in \mathcal{S}} ... \sum_{y_N \in \mathcal{S}} \int_{\mathbb{R}} ... \int_{\mathbb{R}} e^{-\frac{U_G(\vec{x},\vec{y},f)}{K_B T}}\, \mathrm{d}x_1 ... \mathrm{d}x_N. \tag{3}$$

We underline that the use of the spin variables, with the integration over all the phase space, corresponds to a multivalued energy function. This approach must be therefore justified and this is numerically done in the recent literature [30, 33]. We let now $x_1 - x_0 = \xi_1$, $x_2 - x_1 = \xi_2$,..., $x_N - x_{N-1} = \xi_N$, from which we get $x_N = \sum_{j=1}^{N} \xi_j$, with $x_0 = 0$. Hence, we obtain

$$Z_G(f) = \prod_{i=1}^{N} \left\{ \sum_{y_i \in \mathcal{S}} e^{-\frac{v(y_i)}{K_B T}} \mathcal{G}_i \right\}, \tag{4}$$

where

$$\mathcal{G}_i = \int_{\mathbb{R}} \exp\left[-\frac{1}{2}\frac{k_i}{K_B T}(\xi_i - y_i\ell)^2 + \frac{f\xi_i}{K_B T} + \frac{g_i y_i}{K_B T}\right] \mathrm{d}\xi_i. \quad (5)$$

This integral can be straightforwardly evaluated and we get

$$Z_G(f) = (8\pi K_B T)^{N/2}\left(\prod_{i=1}^{N}\frac{1}{\sqrt{k_i}}\right)\exp\left(\frac{Nf^2}{2K_B T k_{\text{eff}}}\right) \quad (6)$$
$$\times \prod_{i=1}^{N}\left[\cosh\left(\frac{\ell f + g_i}{K_B T}\right) + \phi_i \cosh\left(\chi\frac{\ell f + g_i}{K_B T}\right)\right].$$

where $\phi_i = e^{-\frac{\Delta E_i}{K_B T}}$ are the Boltzmann factors calculated with the energy jumps ΔE_i and $1/k_{\text{eff}} = (1/N)\sum_{i=1}^{N}\frac{1}{k_i}$ is the inverse of the effective stiffness. The macroscopic behavior of the chain is described by the force-extension response and by the average value of the spin variables, which can be obtained through the Gibbs partition function as follows [33, 34]

$$\langle x\rangle = K_B T\frac{\partial}{\partial f}\log Z_G, \text{ and } \langle\, y_i\,\rangle = K_B T\frac{\partial}{\partial g_i}\log Z_G. \quad (7)$$

When the external field $\vec{g}$ is zero, these results may be evaluated as follows

$$\langle x\rangle = \frac{Nf}{k_{\text{eff}}} + \ell\sum_{i=1}^{N}\frac{\sinh\left(\frac{\ell f}{K_B T}\right) + \chi\phi_i\sinh\left(\frac{\chi\ell f}{K_B T}\right)}{\cosh\left(\frac{\ell f}{K_B T}\right) + \phi_i\cosh\left(\frac{\chi\ell f}{K_B T}\right)}, \quad (8)$$

$$\langle\, y_i\,\rangle = \frac{\sinh\left(\frac{\ell f}{K_B T}\right) + \chi\phi_i\sinh\left(\frac{\chi\ell f}{K_B T}\right)}{\cosh\left(\frac{\ell f}{K_B T}\right) + \phi_i\cosh\left(\frac{\chi\ell f}{K_B T}\right)}. \quad (9)$$

While the first expression represents the macroscopic mechanical response of the system, the second one describes the configurational state (folded or unfolded) of the units in terms of the applied force. Interestingly enough, Eqs.(8) and (9) can be combined to give $\langle x\rangle = \frac{Nf}{k_{\text{eff}}} + \ell\sum_{i=1}^{N}\langle\, y_i\,\rangle$, which represents a spring-like behavior with the equilibrium length controlled by the spin variables. An application of Eqs.(8) and (9) can be found in Figs.1b, 1c, and 1d, where the force-extension relation, the average spin variables and the quantities $\partial\langle\, y_i\,\rangle/\partial\langle x\rangle$ versus $\langle x\rangle$ are represented for a homogeneous chain with $\Delta E_i = \Delta E\ \forall i$ (blue curves). These results describe a synchronous unfolding of the units for a given threshold force given by $f^* = \Delta E/[(\chi - 1)\ell]$ [18, 33, 42]. It is a well known behavior observed in DNA [12–14], and other molecules of biological origin [43, 44]. A second example can be found in Figs.1j, 1k, and 1l, where the same quantities have been shown for a heterogeneous chain, as represented in Fig.1i. In this case, while the force-extension curve is only slightly modified, the spin variables assume different behaviors for the different units, proving the emergence of an unfolding pathway induced by the heterogeneity of the metastable states energy levels. Also, the blue curve in Fig.1k shows the mean value of the numbered curves and is similar to the Gibbs response of the homogeneous case. This is true since we used the same parameter χ for all the units of the chain. It is important to remark that, for an heterogeneous parameter χ, we can have a different behavior between $\langle y_i\rangle$ of the homogeneous chain and $\frac{1}{N}\sum\langle\, y_i\,\rangle$ of the heterogeneous chain. To conclude, we observe that the quantity $\partial\langle\, y_i\,\rangle/\partial\langle x\rangle$ can be considered as an approximated measure of the probability density of the position x at which a transition occurs between the states of the i-th unit (see below for details). Therefore, Fig.1l confirms the identification of a unfolding sequence induced by the heterogeneity. The analysis of the Gibbs ensemble is the starting point for studying the behavior of the Helmholtz ensemble, which is the core of our investigation as discussed below.

3. The Helmholtz ensemble

We are now interested in the case of a two-state heterogeneous one-dimensional chain within the Helmholtz ensemble (isometric condition imposed by a prescribed extension). To analyze this system, we use the Fourier relation linking the Gibbs and Helmholtz partition functions [45, 46]

$$Z_H(x) = \int_{-\infty}^{+\infty} Z_G(-i\omega K_B T)\exp(i\omega x)\mathrm{d}\omega. \quad (10)$$

Since the direct calculation of $Z_H(x)$ is a very complicated theoretical problem, we use Eq.(10) to determine the mathematical form of $Z_H(x)$ on the base of the analytic continuation of the previously obtained function $Z_G(f)$ (with imaginary values of f) [45, 46]. The aim of this section is to describe the macroscopic behavior of the chain given by the average quantities [33, 34]

$$\langle f\rangle = -K_B T\frac{\partial}{\partial x}\log Z_H, \text{ and } \langle y_j\rangle = K_B T\frac{\partial}{\partial g_j}\log Z_H. \quad (11)$$

Therefore, we develop both Z_H and $\frac{\partial Z_H(x)}{\partial g_j}$ (with $\vec{g} = 0$), as follows

$$Z_H(x) = \int_{-\infty}^{+\infty} e^{-\frac{N\omega^2 K_B T}{2k_{\text{eff}}}} e^{i\omega x}\prod_{i=1}^{N}(a + \phi_i b)\,\mathrm{d}\omega, \quad (12)$$

$$\frac{\partial Z_H(x)}{\partial g_j} = -\frac{i}{K_B T}\int_{-\infty}^{+\infty}\left[\sin\omega\ell + \phi_j\chi\sin\omega\chi\ell\right]$$
$$\times e^{-\frac{N\omega^2 K_B T}{2k_{\text{eff}}}} e^{i\omega x}\prod_{k=1,k\neq j}^{N}(a + \phi_k b)\,\mathrm{d}\omega. \quad (13)$$

where we omitted the unimportant multiplicative constant and we defined $a = \cos\omega\ell$ and $b = \cos\omega\chi\ell$. Hence, we calculate

$$\prod_{i=1}^{N}(a + \phi_i b) = a^N + a^{N-1}b\sum_j\phi_j + a^{N-2}b^2\frac{1}{2}\sum_{i\neq j}\phi_i\phi_j$$
$$+ a^{N-3}b^3\frac{1}{3!}\sum_{i\neq j, i\neq k, j\neq k}\phi_i\phi_j\phi_k$$
$$+ \ldots + b^N\phi_1\times\ldots\times\phi_N = \sum_{k=0}^{N}a^{N-k}b^k S_k, \quad (14)$$

with $S_0 = 1$ and

$$S_k = \frac{1}{k!}\sum_{j_a\neq j_b\,\forall a\neq b}\phi_{j_1}\times\ldots\times\phi_{j_k}. \quad (15)$$

The quantities S_k are called elementary symmetric polynomials in the variables ϕ_1, ..., ϕ_N. To determine S_k, we take the sum of all products of the elements of the k-subsets of the N variables ϕ_1,...,ϕ_N (a k-subset is a subset of a set of N elements containing exactly k elements). Therefore, the sum in Eq.(15) is evaluated over $\binom{N}{k}$ terms. It follows that the direct calculation of these quantities is computationally expensive because of the very large number of permutations. Nevertheless, the complexity can be reduced by introducing the so-called power sums, defined as

$$P_h = \sum_{t=1}^{N} \phi_t^h = \sum_{t=1}^{N} e^{-\frac{h\Delta E_t}{K_B T}}, \tag{16}$$

where, by definition, $P_0 = N$. These quantities can be easily calculated for $h = 1, ..., N$, and the direct relation between the power sums and the elementary symmetric polynomials is given by the following determinant [47, 48]

$$S_k = \frac{1}{k!} \det \begin{bmatrix} P_1 & 1 & 0 & ... & 0 & 0 \\ P_2 & P_1 & 2 & ... & 0 & 0 \\ P_3 & P_2 & P_1 & ... & 0 & 0 \\ ... & ... & ... & ... & ... & ... \\ P_{k-1} & P_{k-2} & P_{k-3} & ... & P_1 & k-1 \\ P_k & P_{k-1} & P_{k-2} & ... & P_2 & P_1 \end{bmatrix}, \tag{17}$$

which can be used to efficiently evaluate the expressions of Z_H and $\frac{\partial Z_H}{\partial g_j}$. The result given in Eq.(17) is an alternative form of the so-called Newton identities or Newton-Girard formulae [49, 50]. Interestingly enough, other relations between the partition function calculation and certain symmetric polynomials have been discussed for ideal quantum gases [51]. We start with the calculation of $Z_H(x)$ and we can write

$$Z_H(x) = \sum_{k=0}^{N} S_k \int_{-\infty}^{+\infty} e^{-\frac{N\omega^2 K_B T}{2k_{\text{eff}}}} e^{i\omega x} a^{N-k} b^k \mathrm{d}\omega. \tag{18}$$

Here, the trigonometric functions in a and b can be expanded through complex exponential functions and the powers can be developed by the binomial theorem. The remaining integral is of the form $\int_{-\infty}^{+\infty} e^{-\alpha x^2} e^{i\beta x} \mathrm{d}x = \sqrt{\frac{\pi}{\alpha}} e^{-\frac{\beta^2}{4\alpha}}$, and therefore we eventually get the first result

$$\begin{aligned} Z_H(x) =& \frac{1}{2^N} \sqrt{\frac{2\pi k_{\text{eff}}}{N K_B T}} \sum_{k=0}^{N} \sum_{s=0}^{N-k} \sum_{q=0}^{k} S_k \binom{N-k}{s} \binom{k}{q} \\ & \times e^{-\frac{k_{\text{eff}}[x+\ell(2s-N+k+2\chi q-\chi k)]^2}{2NK_B T}}, \end{aligned} \tag{19}$$

where the S_k coefficients are calculated by means of Eq.(17). Concerning the calculation of $\frac{\partial Z_H(x)}{\partial g_j}$, we have

$$\begin{aligned} \frac{\partial Z_H(x)}{\partial g_j} =& -\frac{i}{K_B T} \sum_{k=0}^{N-1} S_k^{(j)} \int_{-\infty}^{+\infty} \left[\sin \omega\ell + \phi_j \chi \sin \omega\chi\ell\right] \\ & \times e^{-\frac{N\omega^2 K_B T}{2k_{\text{eff}}}} e^{i\omega x} a^{N-1-k} b^k \mathrm{d}\omega, \end{aligned} \tag{20}$$

where we defined

$$S_k^{(j)} = \frac{1}{k!} \sum_{j_a \neq j_b \forall a \neq b, j_c \neq j \forall c} \phi_{j_1} \times ... \times \phi_{j_k}. \tag{21}$$

The quantities $S_k^{(j)}$ ($k = 1, ..., N-1$) are defined similarly to the quantities S_k ($k = 1, ..., N$) but are based on the set containing all $\phi_1, ..., \phi_N$ except ϕ_j. They can be simply calculated with the same technique based on the determinants, as shown in Eq.(17). We first determine the power sums

$$P_h^{(j)} = \sum_{t=1, t\neq j}^{N} \phi_t^h = \sum_{t=1, t\neq j}^{N} e^{-\frac{h\Delta E_t}{K_B T}}, \tag{22}$$

and then we determine the elementary symmetric polynomials through the following determinant

$$S_k^{(j)} = \frac{1}{k!} \det \begin{bmatrix} P_1^{(j)} & 1 & 0 & ... & 0 & 0 \\ P_2^{(j)} & P_1^{(j)} & 2 & ... & 0 & 0 \\ P_3^{(j)} & P_2^{(j)} & P_1^{(j)} & ... & 0 & 0 \\ ... & ... & ... & ... & ... & ... \\ P_{k-1}^{(j)} & P_{k-2}^{(j)} & P_{k-3}^{(j)} & ... & P_1^{(j)} & k-1 \\ P_k^{(j)} & P_{k-1}^{(j)} & P_{k-2}^{(j)} & ... & P_2^{(j)} & P_1^{(j)} \end{bmatrix}. \tag{23}$$

Straightforward calculations allow to put Eq.(20) in the explicit form

$$\frac{\partial Z_H(x)}{\partial g_j} = \frac{1}{K_B T} \sum_{k=0}^{N-1} \left[\left(\beta_k + \chi\gamma_k\phi_j\right) S_k^{(j)}\right], \tag{24}$$

where the coefficients β_k and γ_k are given by

$$\begin{aligned} \beta_k =& \frac{1}{2^N} \sqrt{\frac{2\pi k_{\text{eff}}}{N K_B T}} \sum_{s=0}^{N-k-1} \sum_{q=0}^{k} \binom{N-k-1}{s} \binom{k}{q} \\ & \times \left[e^{-\frac{k_{\text{eff}}[x+\ell(2s-N+k+2\chi q-\chi k)]^2}{2NK_B T}} - e^{-\frac{k_{\text{eff}}[x+\ell(2s-N+2+k+2\chi q-\chi k)]^2}{2NK_B T}}\right]. \end{aligned} \tag{25}$$

and

$$\begin{aligned} \gamma_k =& \frac{1}{2^N} \sqrt{\frac{2\pi k_{\text{eff}}}{N K_B T}} \sum_{s=0}^{N-k-1} \sum_{q=0}^{k} \binom{N-k-1}{s} \binom{k}{q} \\ & \times \left[e^{-\frac{k_{\text{eff}}[x+\ell(2s-N+1-\chi+k+2\chi q-\chi k)]^2}{2NK_B T}} - e^{-\frac{k_{\text{eff}}[x+\ell(2s-N+1+\chi+k+2\chi q-\chi k)]^2}{2NK_B T}}\right]. \end{aligned} \tag{26}$$

From Eqs.(11) and (19) we can finally determine the force-extension response ($\langle f \rangle$ versus x) as

$$\langle f \rangle = \frac{k_{\text{eff}} \sum_{k=0}^{N} \sum_{s=0}^{N-k} \sum_{q=0}^{k} S_k \binom{N-k}{s} \binom{k}{q} e^{-\frac{k_{\text{eff}}\varphi^2}{2NK_B T}} \varphi_{ksq}}{N \sum_{k=0}^{N} \sum_{s=0}^{N-k} \sum_{q=0}^{k} S_k \binom{N-k}{s} \binom{k}{q} e^{-\frac{k_{\text{eff}}\varphi^2}{2NK_B T}}}, \tag{27}$$

where $\varphi_{ksq} = x + \ell(2s - N + k + 2\chi q - \chi k)$ and the coefficients S_k are given in Eq.(17). Similarly, the expression for the average spin variable $\langle y_j \rangle$ can be obtained from Eqs.(11) and (24) as

$$\langle y_j \rangle = \frac{\sum_{k=0}^{N-1} \left[\left(\beta_k + \chi\gamma_k\phi_j\right) S_k^{(j)}\right]}{Z_H}, \tag{28}$$

where the coefficients $S_k^{(j)}$ are given in Eq.(23).

Although the quenched disorder strongly complicates the analysis of the system within the Helmholtz ensemble, the application of the determinant expression in Eq.(17) or Eq.(23)

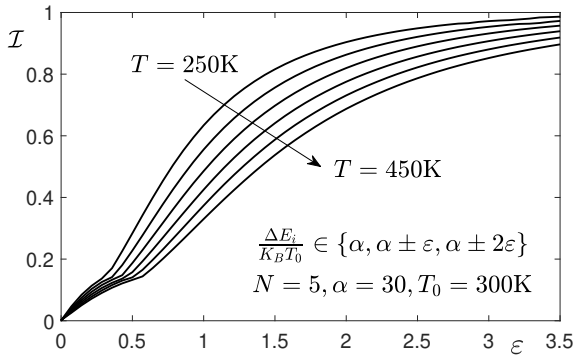

Figure 2: Identifiability $\mathcal{I}$ defined as in Eq.(30) as function of the distribution of the energy jumps ΔE_i (described by the parameter ε) and the temperature T. We adopted the following parameters: $N = 5$, $\ell = 0.5$nm, $T_0 = 300$K, $\chi = 7$, $k_i = 0.04$N/m $\forall i$, $\frac{\Delta E_i}{K_B T_0} \in \{\alpha, \alpha \pm \varepsilon, \alpha \pm 2\varepsilon\}$ with $\alpha = 30$ and ε variable.

(determining the elementary symmetric polynomials S_k or $S_k^{(j)}$ related to the Boltzmann factors with arbitrary energy jumps) allows for an analytic treatment of the problem. In particular, we are able to obtain the partition function in Eq.(19) (along with its derivative in Eq.(24)) in closed form and to derive expressions for the macroscopic observables.

A first simple application of these results can be found in Fig.1b and 1c, where we plot $\langle f \rangle$ and $\langle y_i \rangle$ versus the prescribed extension x for a homogeneous chain under isometric condition (red curves). The behavior of $\langle f \rangle$ and $\langle y_i \rangle$ can be interpreted through a sequential unfolding of the units. This response is in good qualitative agreement with several force-spectroscopy measurements performed on proteins and other macromolecules [52–56]. We also plotted $\partial \langle y_i \rangle / \partial x$ versus x in Fig.1d. This quantity satisfies two crucial properties: firstly, $\int_0^{+\infty} (\partial \langle y_i \rangle / \partial x) dx = \langle y_i \rangle(+\infty) - \langle y_i \rangle(0) = \chi$ (which means that it can be normalized); secondly, $\langle y_i \rangle$ is always non-decreasing, leading to a non-negative function $\partial \langle y_i \rangle / \partial x$. Hence, it follows that $\partial \langle y_i \rangle / \partial x$ can be used as a quantity approximately measuring the probability density of the position x at which a transition occurs between the states of the i-th unit. We remark that it is not a rigorous statement but a useful practical approach to quantify the statistics of the unfolding processes. Fig.1d shows that at each transition occurrence the switching probability is the same for all units of the homogeneous chain. Therefore, no unfolding pathway can be identified.

We describe now the behavior of a heterogeneous chain, as represented in Fig.1e. While the force-extension curve in Fig.1f is slightly modified with respect to Fig.1b, we observe that the heterogeneity of the chain, which is a quenched disorder embedded in the system, is able to perform a symmetry breaking generating an unfolding pathway. Indeed, the numbered curves of the average spin variables in Fig.1g are able to precisely identify what unit is unfolded at each transition, indicating the actual sequence of unfolding processes. Interestingly enough, the red curve in the same panel shows the average value of these numbered curves and is similar to the Helmhotz response of the homogeneous case. This is true since we used the same parameter χ for all the units of the chain. It is important to remark that, for an heterogeneous parameter χ, we can have a different behavior between $\langle y_i \rangle$ of the homogeneous chain and $\frac{1}{N} \sum \langle y_i \rangle$ of the heterogeneous chain. Importantly, it follows that through the spin variables, we can now analyze the unfolding pathway generated by the heterogeneity. This is further confirmed by the plots of $\partial \langle y_i \rangle / \partial x$ in Fig.1h, where each curve is characterized by one pronounced peak corresponding to the actual switching, and other smaller peaks measuring the uncertainty in the pathway identification (see next section for details). Moreover, the numerical results show that the unfolding pathway corresponds to the ascending order of the values ΔE_i. This implies that the equilibrium statistical mechanics of this system implements a statistical sorting procedure. This result is independent of the heterogeneity of the elastic constants k_i since $\langle f \rangle$ and $\langle y_j \rangle$ depend only on the effective stiffness k_{eff}.

4. Unfolding pathway identifiability

While the described identification of the unfolding pathway may seem a simple and expected result, it is important to observe that: (i) the model elaborated mathematically explains how the bistable chain can implement the above introduced statistical sorting procedure, and the same methodology can be also applied to more realistic situations with additional heterogeneous geometrical and/or physical parameters; (ii) the knowledge of the average spin variables given in Eq.(28) is also useful to quantitatively evaluate the identifiability of the most probable unfolding pathway, i.e. of the most likely observed unfolding sequence in a given experiment. This concept measures to what extend we are able to identify the most probable unfolding pathway, which represent the sequence of unfolding process observed the largest number of times if we conduct several identical experiments.

For the sake of brevity, we develop this concept only by considering the Helmholtz ensemble. If we look at the density-like curve $\partial \langle y_i \rangle / \partial x$ for a given unit, see Fig.1h, the identifiability can be defined as the relative difference between the largest peak and the second largest peak. Indeed, this difference measures the capability to properly identify the transition of that unit with respect to the other ones. Consequently, if we consider the i-th unit, we can define

$$\mathcal{I}_i = \frac{\mathcal{F}_m \left\{ \frac{\partial \langle y_i \rangle}{\partial x} \right\} - \mathcal{S}_m \left\{ \frac{\partial \langle y_i \rangle}{\partial x} \right\}}{\mathcal{F}_m \left\{ \frac{\partial \langle y_i \rangle}{\partial x} \right\}}, \tag{29}$$

where $\mathcal{F}_m$ and $\mathcal{S}_m$ are operators extracting the largest peak and the second largest peak, respectively, of a given function. The identifiability of the whole unfolding process can be therefore defined by the average value of these quantities over the N units

$$\mathcal{I} = \frac{1}{N} \sum_{i=1}^{N} \mathcal{I}_i. \tag{30}$$

We first apply this concept to a chain composed of $N = 5$ units with uniformly distributed energy jumps $\Delta E_i / (K_B T) \in \{\alpha, \alpha \pm \varepsilon, \alpha \pm 2\varepsilon\}$, where the parameter ε measures their dispersion. The resulting identifiability $\mathcal{I}$ can be found in Fig.2,

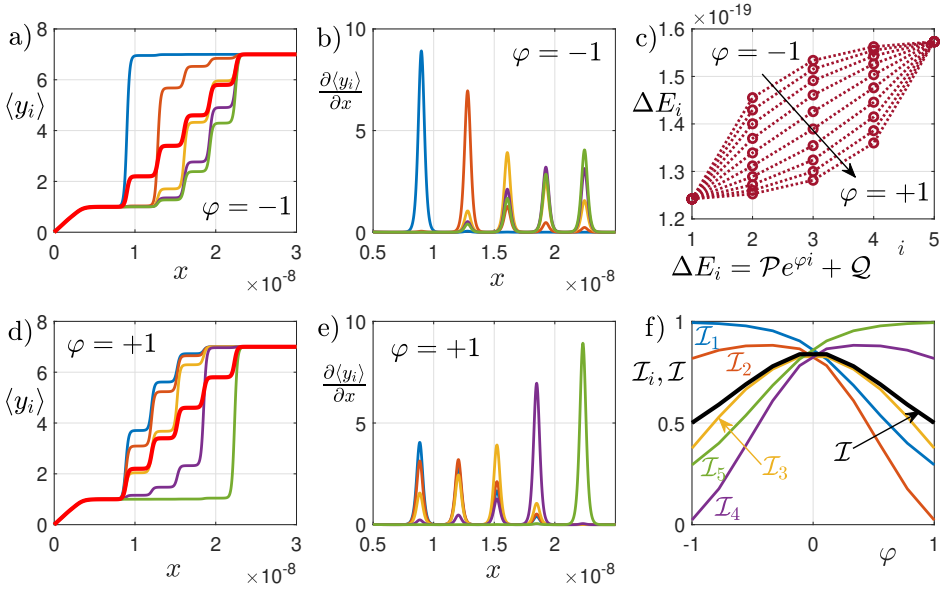

Figure 3: Unfolding pathway in heterogeneous chains with nonuniform distribution of energy jumps. We adopted the distribution $\Delta E_i = \mathcal{P} e^{i\varphi} + \mathcal{Q}$ with $\mathcal{P} = (\Delta E_N - \Delta E_1)/(e^{N\varphi} - e^{\varphi})$ and $\mathcal{Q} = (\Delta E_1 e^{N\varphi} - \Delta E_N e^{\varphi})/(e^{N\varphi} - e^{\varphi})$ (see Eq.(31)). Panels a) and d): average spin variables $\langle y_i \rangle$ for $\varphi = \pm 1$. Panels b) and e): derivatives $\partial \langle y_i \rangle / \partial x$ for $\varphi = \pm 1$. Panel c): distributions of the energy jumps for $-1 \leq \varphi \leq +1$ and with $\Delta E_1 = 30 K_B T$ and $\Delta E_N = \Delta E_5 = 38 K_B T$. Panel f): identifiabilities $\mathcal{I}_i$ and $\mathcal{I}$ versus φ. We adopted the following parameters: $N = 5$, $\ell = 0.5$nm, $T = 300$K, $\chi = 7$, and $k_i = 0.04$N/m $\forall i$.

where it is plotted versus ε and parametrized by the temperature T. We note that $\mathcal{I} = 0$ for the homogeneous case with $\varepsilon = 0$, and $\mathcal{I} \to 1$ for increasing value of ε, being the limiting value $\mathcal{I} = 1$ related to the pathway identification without uncertainty. We also observe that increasing values of the temperature reduce the identifiability, for a constant ε. This is coherent with the idea that the thermal fluctuations are able to reduce the knowledge on the configurational state of the system.

A more complex example deals with a nonlinear distribution of energy jumps of the units. More specifically, we can consider an exponential distribution described by $\Delta E_i = \mathcal{P} e^{i\varphi} + \mathcal{Q}$, where $\mathcal{P}$ and $\mathcal{Q}$ are fixed by imposing the values ΔE_1 and ΔE_N, φ is a free parameter defining the nonlinearity of the energy jumps, and i is the index enumerating the units. It means that the distribution of energy jumps can be written as

$$\Delta E_i = \frac{\Delta E_1 \left(e^{N\varphi} - e^{i\varphi}\right) + \Delta E_N \left(e^{i\varphi} - e^{\varphi}\right)}{e^{N\varphi} - e^{\varphi}}. \qquad (31)$$

As a particular case, we observe that if $\varphi \to 0$, we obtain the linear distribution of energy jumps $\Delta E_i = \Delta E_1 + \Delta E_N (i-1)/(N-1)$, already considered in the previous analysis. The results based on these assumptions can be found in Fig.3. In panels a) and b) one can find the average spin variables and their derivatives, respectively, for the case with $\varphi = -1$. In this case, the energy jumps are given by a nonlinear concave distribution, as plotted in panel c). Similarly, in panels d) and e), we show the results for $\varphi = 1$, corresponding to a nonlinear convex distribution, which is shown in panel c), as well. Finally, in panel f) the identifiabilities are represented for each unit and for the whole chain. It is important to observe that the nonlinearity of the energy jumps is reflected in the spread or dispersion of the values $\mathcal{I}_i$, especially for φ approaching ± 1. Indeed, it is more difficult to identify the unfolding pathway of units with similar energy jumps (see, e.g., $\mathcal{I}_4$ and $\mathcal{I}_5$ for $\varphi = -1$ or $\mathcal{I}_1$ and $\mathcal{I}_2$ for $\varphi = +1$) than the unfolding pathway of units with largely spaced energy jumps (see, e.g., $\mathcal{I}_1$ and $\mathcal{I}_2$ for $\varphi = -1$ or $\mathcal{I}_4$ and $\mathcal{I}_5$ for $\varphi = +1$). We also note that in the limiting case with $\varphi \to 0$, the distribution becomes linear, as previously anticipated, and all the quantities $\mathcal{I}_i$ assume approximately the same value. Coherently, the black curve in panel f), representing the average value $\mathcal{I}$, shows a maximum for $\varphi \to 0$, proving that the largest identifiability is achieved for linearly spaced or distributed energy jumps.

The applicability of the identifiability concept is twofold. From one side, it allows a better understanding of the unfolding pathways of proteins and other bio-macromolecules, typically measured through force-spectroscopy techniques. In particular, it can explain the statistical modifications or variability of the unfolding pathway, which is sometimes depending on several experimental conditions [57–59]. On the other side, the identificability concept may be useful to improve the design of heterogeneous micro- and nano-systems based on bi-and multistability, where folding and unfolding sequences represent the response of the system and should be therefore stable to temperature variations and to other structural or external parameters [60]. The important point for the applications is that the identifiability can be calculated for any set of parameters describing the chain, and allows therefore a parametric analysis of the stability of the most probable unfolding pathway, observed when we conduct several identical experiments. Even if we limited the analysis of the identifiability only to the Helmholtz case, we can compare the two ensembles as follows. From panels h) and l) of Fig.1, it is not difficult to realize that for a fixed chain

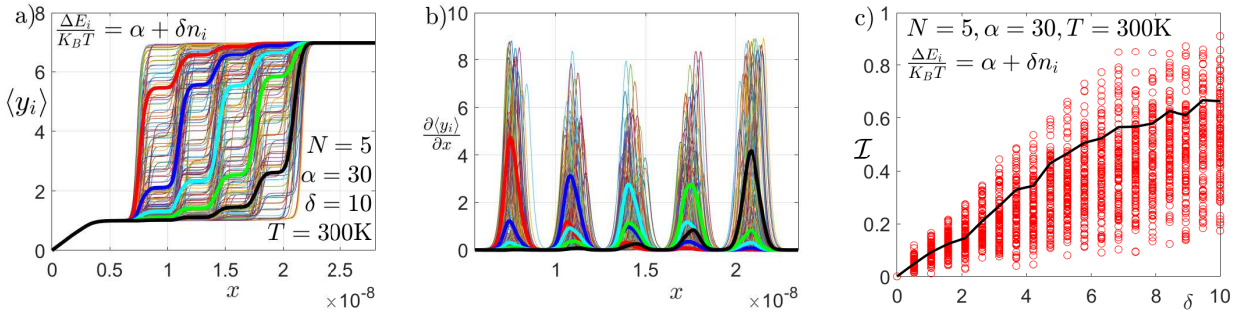

Figure 4: Unfolding pathway in randomly heterogeneous chains. Panel a): average spin variables $\langle y_i \rangle$. Panel b): derivatives $\partial \langle y_i \rangle / \partial x$. In both panels, 50 Monte-Carlo realizations have been plotted (thin lines) together with their average values (thick lines) for a system with $\Delta E_i/(K_B T) = \alpha + \delta n_i$, where n_i are independent and uniform random variables in the interval $(-1, 1)$. Panel c): identifiability $\mathcal{I}$ versus δ. We plotted 100 Monte-Carlo realizations (red circles) and the average value (black solid line). We adopted the following parameters: $N = 5$, $\ell = 0.5$nm, $T = 300$K, $\chi = 7$, $k_i = 0.04$N/m $\forall i$, $\alpha = 30$ and $\delta = 10$ (in panels a) and b) only).

the identifiability in the two ensembles is not the same and the Helmholtz ensemble is capable to maximize this quantity. Indeed, the variance of the peaks in panel l) is much larger than the variance of the peaks in panel h). This result can be easily interpreted in terms of the differences between the Helmholtz and the Gibbs ensemble. As a matter of fact, also for a simple homogeneous chain, in the Gibbs ensemble we have a synchronized unfolding of the units whereas in the Helmholtz ensemble we have a sequential unfolding. Therefore, the Helmholtz unfolding, being sequential, is more adapted to separate the unfolding events and to eventually improve the identifiability.

To conclude this discussion, we determine $\mathcal{I}$ for a bistable chain with random energy jumps between the folded and unfolded states (under isometric conditions). We assume that the energy jumps are given by $\Delta E_i/(K_B T) = \alpha + \delta n_i$, where α and δ are fixed parameters while n_i are independent and uniform random variables in the interval $(-1, 1)$. Of course, the parameter δ measures the stochastic spread of the energy jumps distribution. We generate a given number of chains (Monte-Carlo realizations) using the previous rule to assign the energy jumps of the units. Then, we sort the units in each chain in such a way as to have the energy jumps in ascending order. This is simply useful to easily compare the spin variables of different chains, corresponding to units of the same ordered position. For any chain, we are able to calculate the average spin variables $\langle y_i \rangle$ and their derivatives $\partial \langle y_i \rangle / \partial x$ with respect to the increasing extension x of the chain. Consequently, for each chain, we can determine the corresponding identifiability through Eq.(30). These calculations can be repeated for all generated Monte-Carlo realizations and the means values can be eventually evaluated (sampling Monte-Carlo approach). The results can be found in Fig.4. In panel a) and b) we show the average spin variables $\langle y_i \rangle$ and their derivatives $\partial \langle y_i \rangle / \partial x$, respectively, for 50 Monte-Carlo realizations of the system. The results of the single realizations (thin solid lines) are plotted together with their sample mean values (thick solid lines). We can see that, with the adopted parameters, the average spin variables allow the unfolding pathway identification also with random energy jumps. While panels a) and b) of Fig.4 concern a fixed value of δ, we can perform a more complete analysis where δ is variable over a given range. Hence, being the standard deviation of the energy jumps $\sigma_{\Delta E_i} = K_B T \delta / \sqrt{3}$ proportional to δ, we plot in panel c) the identifiability $\mathcal{I}$ versus δ. We used 100 Monte-Carlo realizations for each value of δ (20 values of δ in the range $[0, 10]$), represented by the red circles in panel c), and we calculated the sample mean values of the identifiability, represented by the solid black line. We repeated the whole protocol several times and we proved that the solid black line, describing the behavior of $\mathcal{I}$, remains stable within an maximal error bar of around ± 0.1. It means that the Monte-Carlo sample with 100 chains is large enough to give acceptable results. We observe that, for random chains, relatively large values of $\delta < \alpha$ are necessary to obtain a good average identifiability of the unfolding path.

5. Conclusions

We considered the statistical and mechanical behavior of heterogeneous chains of bistable units. Since this system is paradigmatically important to represent several situations of practical interest, we thoroughly analyzed its behavior in both isotensional and isometric conditions.

The most important achievement concerns the exact calculation of the partition function (and related quantities) within the Helmholtz ensemble (isometric condition). In this case the heterogeneity represents a quenched disorder, whose analysis is a difficult task of the statistical mechanics. We obtained the closed form expression of the partition function thanks to the Laplace-Fourier relation between Z_H and Z_G [45, 46] and using the determinant form of the so-called Newton-Girard formulae [47–50]. This original approach represents the core of our analysis. We observed that for a homogeneous chain, no unfolded pathway can be identified since all units have the same switching probability at each transition occurrence. On the other hand, the heterogeneity breaks this symmetry and we can identify an unfolded pathway, which is described by the ascending order of the energy jumps between folded and unfolded states of each unit. It means that the system implements a statistical sorting procedure when we simply prescribe an increasing distance between first and last units. Since this process has a statistical character, we can define the concept of identifiability, which measures the capability to identify the most probable unfolding

pathway. This concept has been applied to deterministic (linear and exponential) and random distributions of energy jumps. The results of this work can be applied to the better interpretation of the force spectroscopy measurements of biological macromolecules [57–59] and to the accurate design of micro- and nano-systems based on bistable chains with specific properties [60].

The model introduced in this investigation is rather simple. This choice permits to better discuss the theoretical origin of the unfolding pathway and its statistical character. Nevertheless, the model can be further improved to take into account other relevant physical and geometrical features. For instance, concerning the application to macromolecules, the method here introduced can be generalized to deal with three-dimensional bistable freely jointed chains, which have been recently studied only with homogeneous units [33]. Moreover, the same techniques can be applied to describe the behavior of polymer chains with extensible units [34]. Although we considered here only heterogeneous energy jumps and elastic constants, we envisage to generalize this approach also to other parameters characterizing the units (e.g., ℓ, χ and so on). Further investigations will concern the out-of-equilibrium regime of these systems. Indeed, recent works have provided evidence that the traction velocity applied to the chain with an hard device plays an important role in defining the unfolding pathway [61–64]. Therefore, it is important to fully analyze the interplay between the distribution of energy jumps and the applied traction velocity on the unfolding pathway. To do this the Langevin methodology will be combined with the spin variables technique in order to fully describe the dynamics of the system.

Acknowledgment

We acknowledge the region "Hauts de France" for the financial support under project MEPOFIB. We also thank the anonymous reviewers for their valuable comments on our manuscript.

References

[1] T. R. Strick, M.-N. Dessinges, G. Charvin, N. H. Dekker, J.-F. Allemand, D. Bensimon, V. Croquette, Stretching of macromolecules and proteins, Rep. Prog. Phys. 66 (2003) 1-45.

[2] F. Ritort, Single-molecule experiments in biological physics: Methods and applications, J. Phys. Condens. Matter 18 (2006) R531-R583.

[3] K. C. Neuman, A. Nagy, Single-molecule force spectroscopy: Optical tweezers, magnetic tweezers and atomic force microscopy, Nat. Methods 5 (2008) 491-505.

[4] S. Kumar, M. S. Li, Biomolecules under mechanical force, Phys. Rep. 486 (2010) 1-74.

[5] H. Miller, Z. Zhou, J. Shepherd, A.J.M. Wollman, M.C. Leake, Single-molecule techniques in biophysics: A review of the progress in methods and applications, Rep. Prog. Phys. 81 (2018) 024601.

[6] T.E. Fisher, A.F. Oberhauser, M. Carrion-Vazquez, P.E. Marszalek, J.M. Fernandez, The study of protein mechanics with the atomic force microscope, Trends Biochem. Sci. 24 (1999) 379-384.

[7] H. Li, A.F. Oberhauser, S.B. Fowler, J. Clarke, J.M. Fernandez, Atomic force microscopy reveals the mechanical design of a modular protein. Proc. Nat. Acad. Sci. USA 97 (2000) 6527.

[8] G. Florio, G. Puglisi, Unveiling the influence of device stiffness in single macromolecule unfolding, Scientific Reports 9 (2019) 4997.

[9] M. Bonin, R. Zhu, Y. Klaue, J. Oberstrass, E. Oesterschulze, W. Nellen, Analysis of RNA flexibility by scanning force spectroscopy, Nucleic Acids Res. 30 (2002) e81.

[10] J. Lipfert, G.M. Skinner, J.M. Keegstra, T. Hensgens, T. Jager, D. Dulin, M. Köber, Z. Yu, S.P. Donkers, F.-C. Chou, R. Das, N. H. Dekker, Double-stranded RNA under force and torque: Similarities to and striking differences from double-stranded DNA, Proc. Natl. Acad. Sci. USA 111 (2014) 15408.

[11] S.B. Smith, L. Finzi, C. Bustamante, Direct mechanical measurements of the elasticity of single DNA molecules by using magnetic beads, Science 258 (1992) 1122.

[12] J.F. Marko, E.D. Siggia, Stretching DNA, Macromolecules 28 (1995) 8759-8770.

[13] S.M. Smith, Y. Cui, C. Bustamante, Overstretching B-DNA: The Elastic Response of Individual Double-Stranded and Single-Stranded DNA Molecules, Science 271 (1996) 795.

[14] K.R. Chaurasiya, T. Paramanathan, M.J. McCauley, M.C. Williams, Biophysical characterization of DNA binding from single molecule force measurements, Phys. Life Rev. 7 (2010) 299-341.

[15] O.K. Dudko, Decoding the mechanical fingerprints of biomolecules, Q. Rev. Biophys. 49 (2016) 1-14.

[16] M. Rief, J.M. Fernandez, H.E. Gaub, Elastically Coupled Two-Level Systems as a Model for Biopolymer Extensibility, Phys. Rev. Lett. 81 (1998) 4764.

[17] F. Manca, S. Giordano, P. L. Palla, F. Cleri, L. Colombo, Theory and Monte Carlo simulations for the stretching of flexible and semiflexible single polymer chains under external fields, J. Chem. Phys. 137 (2012) 244907.

[18] F. Manca, S. Giordano, P. L. Palla, F. Cleri, L. Colombo, Two-state theory of single-molecule stretching experiments, Phys. Rev. E 87 (2013) 032705.

[19] S. Giordano, Helmholtz and Gibbs ensembles, thermodynamic limit and bistability in polymer lattice models, Continuum Mech. Thermodyn. 30 (2018) 459.

[20] M. Caruel, L. Truskinovsky, Physics of muscle contraction, Rep. Prog. Phys. 81 (2018) 036602.

[21] M. Caruel, P. Moireau, D. Chapelle, Stochastic modeling of chemical–mechanical coupling in striated muscles, Biomechanics and Modeling in Mechanobiology 18 (2019) 563-587.

[22] A. Rafsanjani, D. Pasini, Bistable auxetic mechanical metamaterials inspired by ancient geometric motifs, Extreme Mechanics Letters 9 (2016) 291-296.

[23] S. Katz, S. Givli, Solitary waves in a bistable lattice, Extreme Mechanics Letters 22 (2018) 106-111.

[24] H. Fang, K. W. Wang, S. Li, Asymmetric energy barrier and mechanical diode effect from folding multi-stable stacked-origami, Extreme Mechanics Letters 17 (2017) 7-15.

[25] S. Liu, A. I. Azad, R. Burgueño, Architected materials for tailorable shear behavior with energy dissipation, Extreme Mechanics Letters 28 (2019) 1-7.

[26] I. Müller, P. Villaggio, A model for an elastic-plastic body, Arch. Ration. Mech. Anal. 65 (1977) 25.

[27] B. Fedelich, G. Zanzotto, Hysteresis in discrete systems of possibly interacting elements with a double-well energy, J. Nonlinear Sci. 2 (1992) 319-342.

[28] G. Puglisi, L. Truskinovsky, Thermodynamics of rate-independent plasticity, J. Mech. Phys. Sol. 53 (2005) 655.

[29] M. Caruel, J.-M. Allain, L. Truskinovsky, Mechanics of collective unfolding, J. Mech. Phys. Sol. 76 (2015) 237.

[30] Y.R. Efendiev, L. Truskinovsky, Thermalization of a driven bi-stable FPU chain, Continuum Mech. Thermodyn. 22 (2010) 679.

[31] A. Mielke, L. Truskinovsky, From Discrete Visco-Elasticity to Continuum Rate-Independent Plasticity: Rigorous Results, Arch. Ration. Mech. Anal. 203 (2012) 577-619.

[32] I. Benichou, S. Givli, Structures undergoing discrete phase transformation, J. Mech. Phys. Sol. 61 (2013) 94.

[33] S. Giordano, Spin variable approach for the statistical mechanics of folding and unfolding chains, Soft Matter 13 (2017) 6877-6893.

[34] M. Benedito, S. Giordano, Thermodynamics of small systems with conformational transitions: The case of two-state freely jointed chains with extensible units, J. Chem. Phys. 149 (2018) 054901.

[35] M. Benedito, S. Giordano, Isotensional and isometric force-extension response of chains with bistable units and Ising interactions, Phys. Rev. E 98 (2018) 052146.
[36] M. Benedito, S. Giordano, Full Statistics of Conjugated Thermodynamic Ensembles in Chains of Bistable Units, Inventions 4 (2019) 19.
[37] M. Caruel, J. M. Allain, L. Truskinovsky, Muscle as a Metamaterial Operating Near a Critical Point, Phys. Rev. Lett. 110 (2013) 248103.
[38] M. Caruel, L. Truskinovsky, Statistical mechanics of the Huxley-Simmons model, Phys. Rev. E 93 (2016) 062407.
[39] L. Truskinovsky, A. Vainchtein, The origin of nucleation peak in transformational plasticity, J. Mech. Phys. Sol. 52 (2004) 1421.
[40] G. Puglisi, Hysteresis in multi-stable lattices with non-local interactions, J. Mech. Phys. Sol. 54 (2006) 2060.
[41] H. A. Kramers, Brownian motion in a field of force and the diffusion model of chemical reactions, Physica 7 (1940) 284-304.
[42] G. I. Bell, Models for the specific adhesion of cells to cells, Science 200 (1978) 618-627.
[43] M. S. Z. Kellermayer, S. B. Smith, H. L. Granzier, C. Bustamante, Folding-Unfolding Transitions in Single Titin Molecules Characterized with Laser Tweezers, Science 276 (1997) 1112-1116.
[44] J. Zakrisson, K. Wiklund, M. Servin, O. Axner, C. Lacoursière, M. Andersson, Rigid multibody simulation of a helix-like structure: the dynamics of bacterial adhesion pili, Eur. Biophys. J.44 (2015) 291-300.
[45] F. Manca, S. Giordano, P. L. Palla, R. Zucca, F. Cleri, L. Colombo, Elasticity of flexible and semiflexible polymers with extensible bonds in the Gibbs and Helmholtz ensembles, J. Chem. Phys. 136 (2012) 154906.
[46] F. Manca, S. Giordano, P. L. Palla, F. Cleri, On the equivalence of thermodynamics ensembles for flexible polymer chains, Phys. A Stat. Mech. Its Appl. 395 (2014) 154-170.
[47] H. W. Tumbull, Theory of Equations, Oliver and Boyd, Edinburgh and London, 1947.
[48] H. W. Gould, The Girard-Waring power sum formulas for symmetric functions and Fibonacci sequences, Fibonacci Quart. 37 (1999) 135-140.
[49] D. G. Mead, Newton's Identities, Amer. Math. Monthly 99 (1992) 749-751.
[50] D. Kalman, A Matrix Proof of Newton's Identities, Math. Mag. 73 (2000) 313-315.
[51] H.-J. Schmidt, J. Schnack, Partition functions and symmetric polynomials, Am. J. Phys. 70 (2002) 53-57.
[52] M. Rief, M. Gautel, F. Oesterhelt, J. M. Fernandez, H. E. Gaub, Reversible unfolding of individual titin immunoglobulin domains by AFM, Science 276 (1997) 1109-1112.
[53] D. B. Staple, S. H. Payne, A. L. C. Reddin, H. J. Kreuzer, Stretching and unfolding of multidomain biopolymers: A statistical mechanics theory of titin, Phys. Biol. 6 (2009) 025005.
[54] A. Prados, A. Carpio, L. L. Bonilla, Sawtooth patterns in force-extension curves of biomolecules: An equilibrium-statistical-mechanics theory, Phys. Rev. E 88 (2013) 012704.
[55] L. L. Bonilla, A. Carpio, A. Prados, Theory of force-extension curves for modular proteins and DNA hairpins. Phys. Rev. E 91 (2015) 052712.
[56] D. De Tommasi, N. Millardi, G. Puglisi, G. Saccomandi, An energetic model for macromolecules unfolding in stretching experiments, J. R. Soc. Interface 10 (2013) 20130651.
[57] S. W. Englander, L. Mayne, The case for defined protein folding pathways, Proc. Nat. Acad. Sci. USA 114 (2017) 8253-8258.
[58] M. Yang, B. Yordanov, Y. Levy, R. Brüschweiler, S. Huo, The Sequence-Dependent Unfolding Pathway Plays a Critical Role in the Amyloidogenicity of Transthyretin, Biochemistry 45 (2006) 11992-12002.
[59] A. Yadav, S. Paul, R. Venkatramani, S. R. K. Ainavarapu, Differences in the mechanical unfolding pathways of apo- and copper-bound azurins, Scientific Reports 8 (2018) 1989.
[60] M. Caruel and L. Truskinovsky, Bi-stability resistant to fluctuations, J. Mech. Phys. Sol. 109 (2017) 117.
[61] M. S. Li, and M. Kouza, Dependence of protein mechanical unfolding pathways on pulling speeds, J. Chem. Phys. 130 (2009) 145102.
[62] C. Guardiani, D. Di Marino, A. Tramontano, M. Chinappi, F. Cecconi, Exploring the Unfolding Pathway of Maltose Binding Proteins: An Integrated Computational Approach, J. Chem. Theory Comput. 10 (2014) 3589-3597.
[63] C. A. Plata, F. Cecconi, M. Chinappi, A. Prados, Understanding the dependence on the pulling speed of the unfolding pathway of proteins, J. Stat. Mech. (2015) P08003.
[64] C. A. Plata, Z. N. Scholl, P. E. Marszalek, A. Prados, Relevance of the Speed and Direction of Pulling in Simple Modular Proteins, J. Chem. Theory Comput. 14 (2018) 2910-2918.